JOURNAL OF BACTERIOLOGY, Feb. 2001, p. 1284–1295 Vol. 183, No. 4
0021-9193/01/$04.00+0 DOI: 10.1128/JB.2001.183.4.1284–1295.2001

Cloning of the *sodA* Gene from *Corynebacterium melassecola* and Role of Superoxide Dismutase in Cellular Viability

MURIEL MERKAMM AND ARMEL GUYONVARCH*

Institut de Génétique et Microbiologie, Université Paris-Sud, Centre d'Orsay, F-91405 Orsay Cedex, France

Received 9 August 2000/Accepted 16 November 2000

The *sodA* gene encoding the *Corynebacterium melassecola* manganese-cofactored superoxide dismutase (SOD) has been cloned in *Escherichia coli* and sequenced. The gene is transcribed monocistronically; the predicted polypeptide is 200 amino acids long and associates in a homotetrameric, manganese-dependent form, able to complement an SOD-deficient *E. coli* mutant. A second open reading frame, coding for a putative 217-amino-acid protein with high homology to peptide methionine sulfoxide reductases from various origins, has been identified immediately upstream of *sodA* in the opposite transcription orientation. The *sodA* gene was inactivated by insertion of an integrative vector carrying a kanamycin resistance gene. The growth rate of the SOD-deficient integrant was only slightly affected in BHI rich medium as well as in BMCG chemically defined medium, but was strongly affected by the presence of the redox-cycling agent paraquat. The SOD deficiency had, on the other hand, a deleterious effect on viability as soon as the culture entered the stationary phase of growth in BHI medium. Surprisingly, SOD deficiency was able to rescue the dramatic loss of viability observed for the wild-type strain in BMCG synthetic medium when glucose was not the limiting growth factor.

Reactive oxygen species are formed in aerobic organisms as by-products of normal metabolism, as a consequence of partial reduction of molecular oxygen to superoxide anion ($O_2^{\cdot -}$), hydrogen peroxide (H_2O_2), and hydroxyl radical ($^{\cdot}OH$). To protect cells from damage by these reactive species to DNA, proteins, and lipids, aerobic organisms have evolved detoxification and repair systems (69). Superoxide dismutase (SOD; EC 1.15.1.1) is considered a key enzyme in oxygen defense systems by catalyzing the dismutation of $O_2^{\cdot -}$ into oxygen and H_2O_2 (22), the latter being broken in turn to water by catalase or peroxidase.

SODs are classified in different groups depending on the type of metal cofactors: copper-and zinc-containing (Cu,Zn-SOD) (46), iron-containing (Fe-SOD) (83), manganese-containing (Mn-SOD) (39), and nickel-containing (Ni-SOD) (84) enzymes. Another type of small metalloprotein with superoxide dismutase activity, unrelated to classical SODs, has also been recently identified in the sulfate-reducing bacterium *Desulfovibrio* (65). Most bacteria possess an Mn-SOD or an Fe-SOD in their cytoplasm, while Cu,Zn-SODs have been identified in the periplasm or periphery of pathogenic and endosymbiotic bacteria (4, 5, 80). The Mn- and Fe-SODs have highly similar sequences and structures, usually have a strict metal selectivity, and are evolutionarily unrelated to other SODs. On the other hand, some SODs have been found to be active with either manganese or iron incorporated into the same apoprotein (47, 63, 82). These enzymes were named cambialistic. Some bacteria, like *Escherichia coli* and *Pseudomonas aeruginosa*, have both an Fe-SOD and an Mn-SOD, which differ not only in their primary sequences but also in their regulation (29, 72) and, at least for *E. coli*, in their intracellular localization, the Fe-SOD being located closer to the inner membrane than the Mn-SOD enzyme (32).

With the exception of *E. coli*, which has been investigated in detail (72), little is known about bacterial SOD expression and regulation, especially in gram-positive bacteria, although many genes have been cloned and sequenced. Most work concerns pathogenic species, mainly because of the relationship between antioxidant defenses and pathogenicity (1, 4, 85). Less is known about their nonpathogenic relatives. Although the amino acid-producing, telluric, and nonpathogenic *Corynebacteria* species have been well studied for decades, most of the work has focused on biochemical pathways or metabolic fluxes, and nothing is known about their antioxidant defenses. The so-called "amino acid-producing corynebacteria" group contains the closely related *Corynebacterium glutamicum*, *Corynebacterium melassecola*, *Brevibacterium flavum*, and *Brevibacterium lactofermentum* species (42), sometimes gathered together under the sole *C. glutamicum* name, and belongs to the actinomycetes suborder along with the *Mycobacterium* and *Nocardia* genera (66). Considering the high oxygen requirement of the aerobic *C. melassecola* species (15), we found it of great interest to study their antioxidant defenses. We therefore investigated and characterized the *sodA* gene and the corresponding protein of *C. melassecola* and studied the role of this gene in the response to superoxide and in survival after starvation.

MATERIALS AND METHODS

Bacterial strains and growth conditions. The bacterial strains and vectors used in this study are listed in Table 1. *C. melassecola* strains were grown aerobically (250 rpm) at 34°C, either in brain heart infusion (BHI; Difco) rich medium or in BMCG chemically defined medium containing 2% glucose, as described by Guillouet and Engasser (26). Growth was followed by measuring the optical density at 570 nm (OD_{570}) in a DU 7400 Beckman spectrophotometer. Kanamycin (25 μg/ml) and chloramphenicol (6 μg/ml) were added to the medium when needed. The *E. coli* DH5α strain was used for molecular biology procedures. *E. coli* QC1799 *sodA sodB* and its parental GC4468 strain were kindly provided by Danièle Touati (Institut Jacques Monod, Université Paris VII, Paris,

* Corresponding author. Mailing address: Institut de Génétique et Microbiologie, Bat. 360, Université Paris-Sud, Centre d'Orsay, F-91405 Orsay Cedex, France. Phone: 33 (0)1 69 15 63 41. Fax: 33 (0)1 69 15 63 34. E-mail: armel@igmors.u-psud.fr.

TABLE 1. Bacterial strains and plasmids used in this study

Strain or plasmid	Characteristics	Source[a] or reference
C. melassecola		
ATCC 17965	Wild-type strain	ATCC
CGL10016	ATCC 17965 *sodA*::viMM12 (Km^r)	This study
E. coli		
DH5α	F^- Δ(*lac-argF*)*U169 recA1 endA1 hsdR* (r_K^- m_K^+) *supE44 gyrA1 relA1 deoR thi-1* (Φ80d*lacZ*ΔM15)	BRL
GC4468	F^- Δ(*lac-argF*)*U169 rpsL*	73
QC1799	F^- Δ(*lac-argF*)*U169 rpsL* Δ*sodA3*, Φ(*sodB-kan*)Δ2	73
Plasmids		
pGEM-T	Cloning vector for PCR fragments, ColE1 origin, Ap^r	Promega
pMM7	pGEM-T with 0.29-kb S1/S3 amplified fragment from *C. melassecola*, Ap^r	This study
pUN121	Cloning vector, ColE1 origin, Ap^r Tc^s	53
pMM8	pUN121 with 10-kb *C. melassecola* insertion including *sodA*, Ap^r Tc^r	This study
pCGL243	Shuttle vector, pACYC184 origin for *E. coli*, pBL1 origin for *C. melassecola*, Km^r	59
pMM12	pCGL243 with a 0.36-kb *Bam*HI-*Hin*dIII fragment internal to *sodA* (S6/S7 amplification fragment), Km^r	This study
pKK388-1	*E. coli* expression vector with *trc* promoter, Ap^r	11
pCGL482	Shuttle vector, pACYC184 origin for *E. coli*, pBL1 origin for *C. melassecola*, Cm^r	57
pMM23	pCGL482 with the *sodA* gene on a 0.8-kb *Nco*I-*Sma*I fragment from pMM8, under the *trc* promoter as a *Bam*HI-*Nco*I fragment from pKK388-1, Cm^r	This study
viMM12	Integrative vector derived from pMM12 by *Not*I digestion and religation of the 1.8-kb fragment carrying *aphIII* and the internal *sodA* fragment, Km^r	This study

[a] ATCC, American Type Culture Collection, Rockville, Md.; BRL, Bethesda Research Laboratory, Gaithersburg, Md.; Promega Corporation, Madison, Wis.

France). *E coli* strains were grown aerobically at 37°C in Luria-Bertani (LB) medium (Difco) or in M63 glucose minimal medium as described by Carlioz and Touati (13). Growth was monitored at 600 nm (OD_{600}). Ampicillin (100 μg/ml), kanamycin (25 μg/ml), and chloramphenicol (30 μg/ml) were added to the medium when needed. All chemicals were purchased from Sigma.

***C. melassecola*-specific microbial procedures.** Sensitivity to paraquat and hydrogen peroxide (H_2O_2) was monitored by growth inhibition on plates. Bacteria were grown in liquid BHI rich medium to late log phase, and 100-μl aliquots from a 1,000-fold dilution were spread on BHI agar plates. A 5-mm sterile filter paper disk was placed in the middle of each plate and impregnated with 10 μl of 10-mg/ml paraquat or 10% H_2O_2. After 2 days of incubation at 34°C, sensitivity was determined by measuring the diameter of the growth inhibition zone surrounding the disk. For the determination of bacterial viability, *C. melassecola* cultures were serially diluted at room temperature in NaCl (0.9 g/liter), and aliquots were spread on BHI plates. After 2 days of incubation at 34°C, the colonies were counted, and viability was calculated as CFU per OD_{570} unit (CFU/OD).

General molecular biology techniques. Standard molecular biology procedures were used according to Sambrook et al. (62). Enzymes were obtained from Promega and Boehringer Mannheim. Plasmid DNA was prepared with the Wizard kit from Promega, with 1 h of pretreatment at 37°C for *C. melassecola* in Wizard resuspension solution containing lysozyme (20 mg/ml). DNA fragments were isolated from agarose gels with the Jetsorb kit (Genomed). Preparation of *C. melassecola* genomic DNA and Southern blotting were performed as described elsewhere (59). DNA probes were labeled with [α-^{32}P]dCTP (Amersham) using the T7 Quick Prime random priming kit (Pharmacia).

Total *C. melassecola* RNA was prepared from cells grown until the late exponential phase as described by Igo and Losick (34). For Northern blot analysis, approximately 10 μg of RNA was separated on a 1% agarose gel with the RNA ladder (Promega) as size markers. Transfer to a Hybond-N (Amersham) membrane, probe labeling, and hybridization at 65°C without formamide were done as described by Sambrook et al. (62). The probe used for *sodA* transcript monitoring was the PCR fragment isolated from pMM7 (see below). Methylene blue staining of RNAs on blots was performed according to Wilkinson et al. (78).

Cloning of the *sodA* gene. (i) Amplification of an internal fragment by PCR. For PCR experiments, primers S1 [5′-GGCCACACCAACCACTCCGT(C/G)TT-3′] and S3 [5′-AGGTAGAA(A/T)GCGTGCTCCCACAT-3′] (see Fig. 3) were chosen on the basis of highly conserved regions in bacterial Fe- and Mn-SODs (30) and according to the codon preference in *Corynebacterium*-related species (45). PCR was carried out with 2.5 U of thermostable DNA polymerase (AmpliTaqGold; Perkin-Elmer) in a reaction mixture containing 30 ng of genomic *C. melassecola* DNA, 0.2 mM each deoxynucleotide triphosphates (Promega), 0.5 μM each of both primers, 2 mM $MgCl_2$, and 1× AmpliTaqBuffer in a final volume of 50 μl. For the amplification reaction, after 10 min at 94°C, 35 identical cycles (1 min at 94°C, 1 min at 50°C, and 1 min at 72°C) were followed by a final elongation step of 5 min at 72°C. The amplified DNA fragment of the expected size was cloned into the pGEM-T vector (Promega) to give plasmid pMM7. Partial sequencing of the insertion showed high homology with known Fe- and Mn-SODs.

(ii) Cloning of the entire *sodA* gene. The amplified fragment isolated from pMM7 was radiolabeled and used as a probe for colony hybridization (62). One clone (pMM8) was selected from a previously described *C. melassecola* ATCC 17965 genomic library (59). The pMM8 plasmid was shown to carry a 10-kb inserted DNA fragment. From Southern experiments, this DNA fragment clearly originated from the *C. melassecola* chromosomal DNA, without detectable structural alteration. The DNA sequence was determined for 2.2 kb on both stands by primer walking in the region covering the *sodA* gene, using an ABI model 373 DNA sequencer (Applied Biosystem).

Disruption of the *sodA* chromosomal gene. An internal *sodA* fragment (see Fig. 3) was amplified by PCR using primers S6 (5′-GCAGGATCCAACGCAGCACTCGAGGCACTA-3′), including a *Bam*HI site (underlined), and S7 (5′-ATCAAGCTTCAGAACTGGGGTGATGTCGAT-3′), including an *Hin*dIII site (underlined). The 371-bp PCR fragment was digested with *Bam*HI and *Hin*dIII and inserted into the *E. coli-C. melassecola* shuttle vector pCGL243 (59) to create pMM12. This vector was used to construct the integron, essentially as described by Reyes et al. (59). The pMM12 plasmid was introduced into *C. melassecola* by electroporation (9). Plasmid pMM12 was extracted from this host and digested by *Not*I. The 1.8-kb fragment containing the *aphIII* kanamycin resistance gene and the internal *sodA* fragment was isolated and self-ligated to create the viMM12 integron. Transformants from *C. melassecola* wild-type strain with the integron were the result of a single crossing-over, as verified by Southern blotting. The disrupted strain was named CGL10016, and two independant integrants were used for physiological analysis.

Construction of an expression vector for *C. melassecola sodA*. The *trc* promoter was isolated from pKK388-1 (11) as a 0.36-kb *Bam*HI-*Nco*I fragment, and *sodA* was isolated from pMM8 as a 0.8-kb *Nco*I-*Sma*I fragment, including the entire open reading frame (ORF) and the putative terminator (see Fig. 3). The two fragments were ligated together and inserted into a *Bam*HI-*Sma*I-digested pCGL243 shuttle vector to give plasmid pMM23.

Preparation of crude extracts. Bacterial cells were harvested and resuspended in 50 mM sodium phosphate buffer (pH 7.8) to 50 OD_{570} units for *C. melassecola*. Cells were disrupted by vortexing three times 1 ml of suspension with 1 g of 0.5-mm glass beads for 2 min in a 2-ml Eppendorf tube. The suspension was centrifuged at 10,000 × *g* for 15 min, and the resulting supernatant was used as

the crude extract for enzymatic determinations. The protein concentration was measured by the method of Lowry et al. (44) using bovine immunoglobulin G as a standard.

Determination of SOD, catalase, aconitase, and isocitrate dehydrogenase activities. SOD specific activity was determined by the method of Ukeda et al. (74) based on the inhibition of a tetrazolium salt reduction by superoxide generated from a xanthine-xanthine oxidase reaction. Purified *E. coli* Mn-SOD (Sigma) was used as a standard, and 1 U is defined as the amount of enzyme that inhibits the rate of reduction of cytochrome *c* by 50% in the standard xanthine oxidase/cytochrome *c* assay. SOD activity in nondenaturing 10% acrylamide gels was visualized by tetrazolium negative staining according to Schmidt et al. (64). Catalase activity was determined according to Goldberg and Hochman (24) by measuring the disappearance of H_2O_2 at 240 nm, with an initial concentration of 20 mM. *Aspergillus niger* catalase (Sigma) was used as a standard, and 1 U is defined as the amount of enzyme catalyzing the dismutation of 1 μmol of H_2O_2 per min. Aconitase and isocitrate dehydrogenase activities were determined as described by Hanson and Cox (28).

Purification of SOD from *C. melassecola*. One liter of bacterial culture in BHI medium was harvested at an OD_{570} of 8.5, washed twice in 0.5 volume of 25 mM sodium phosphate (pH 7.5) buffer, and resuspended in 40 ml of the same buffer containing 10 mM $MgCl_2$, RNase A (1 μg/ml), and DNase I (1 μg/ml). Cells were disrupted in a French press (SLM Aminco) at 16,000 lb/in^2. The extract was centrifuged at 10,000 × *g* for 15 min at 4°C. The supernatant was ultracentrifuged at 130,000 × *g* for 2 h at 4°C, and the resulting supernatant was used as the cytosoluble fraction. This supernatant was fractionated with ammonium sulfate. Proteins precipitating in the range of 90 to 100% ammonium sulfate saturation, the fraction containing most of the SOD activity, were collected by centrifugation, dissolved in 50 mM Tris-Cl (pH 8.0) buffer, dialyzed against the same buffer, and applied to a Bioscale Q2 (Bio-Rad) ion-exchange column equilibrated with the same buffer. Proteins were eluted with a linear gradient of 0 to 0.5 M NaCl in the same buffer. The most active fractions were pooled, dialyzed against the Tris-Cl (pH 8.0) buffer, and run on a Sephacryl S300 (Pharmacia) column equilibrated with the same buffer. The fractions containing the eluted SOD were pooled and concentrated with a Centriprep-30 (Amicon). After this step, 5 μg of protein was analyzed for purity. After sodium dodecyl sulfate-polyacrylamide gel electrophoresis (SDS-PAGE) and Coomassie blue staining according to Laemmli (40), only a single band could be observed (see Fig. 2).

The molecular mass of the purified native SOD was estimated by gel filtration on Sephacryl S300 using chymotrypsinogen (25 kDa), ovalbumin (45 kDa), bovine serum albumin (68 kDa), and aldolase (158 kDa) as molecular mass markers. The molecular mass of the monomeric protein was estimated by SDS-PAGE using LMW markers (Pharmacia) as molecular mass markers.

The N-terminal sequence of the purified enzyme and sequences from internal fragments generated by trypsin digestion were determined with an ABI model 473A protein sequencer.

Atomic absorption for the identification of the metal cofactor present in the purified SOD was carried out on a Perkin Elmer 2280 atomic absorption spectrometer.

Nucleotide sequence accession number. The assigned accession number for the nucleotide and deduced amino acid sequences of *sodA* and *msrA* is AF236111 in the GenBank nucleotide sequence database.

RESULTS

Heterologous expression of the cloned gene. The *C. melassecola sodA* gene was cloned, through a PCR-based method, as a pMM8-borne DNA fragment as described in Materials and Methods. Since many *C. melassecola* genes have been proven to be expressed in *E. coli* (56), the cloned DNA fragment was tested for its ability to complement the QC1799 *sodA sodB* mutant of *E. coli*. This mutant cannot grow aerobically in minimal medium without addition of a subset of amino acids and exhibits enhanced sensitivity to the superoxide generator paraquat (13). The QC1799 *E. coli* mutant was transformed with plasmid pMM8. The resulting transformed strain showed a growth pattern in minimal medium similar to that of the parental strain. To ensure that *E. coli* complementation depended only on *C. melassecola sodA* gene expression, and for further expression studies in *C. melassecola*, the *sodA* coding region, identified after DNA sequencing (see below), was placed under the control of the *E. coli* hybrid *trc* promoter, which was previously shown to promote efficient expression of genes in both *E. coli* (11) and *C. glutamicum* (17). The resulting pMM23 plasmid was used to transform QC1799, and the recombinant strain showed a growth pattern in minimal medium (Fig. 1a) and in LB medium containing 50 μM paraquat (Fig. 1b) similar to that of the parental SOD-proficient strain and grew even faster than the nontransformed *E. coli* SOD-deficient strain in LB without paraquat (Fig. 1b).

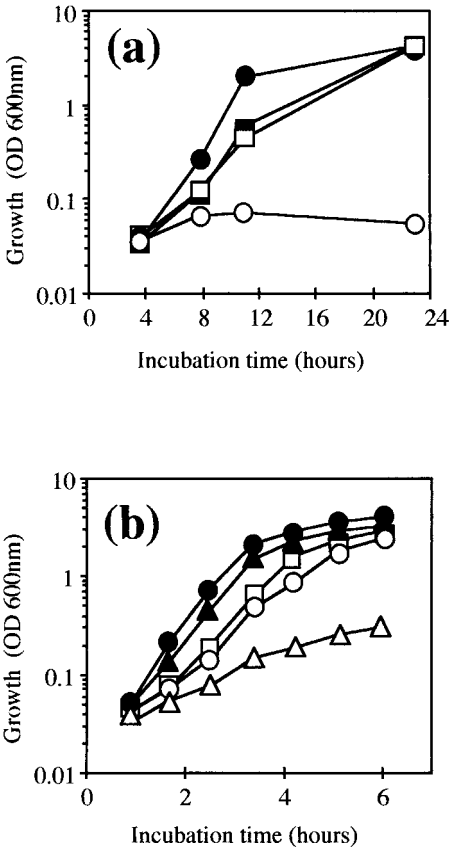

FIG. 1. Complementation of SOD defect in *E. coli* by the *C. melassecola sodA* gene. (a) Growth in M63 minimal medium was measured by OD_{600} for the QC1799 *sodA sodB* mutant transformed by the control vector pCGL482 (○), for QC1799 transformed by pMM23 (□), for the nontransformed parental strain GC4468 (●), and for GC4468 transformed by pMM23 (■). Transformed strains were grown in the presence of chloramphenicol (30 μg/ml). (b) Growth of GC4468 (●, ▲), nontransformed QC1799 (○, △), and QC1799 transformed by pMM23 (□) was monitored by OD_{600} in LB medium in the presence (▲, △, □) or absence (●, ○) of 30 μM paraquat.

SOD specific activity was determined in cell extracts from transformed and nontransformed strains. Activities from GC4468, QC1799, QC1799(pMM8), and QC1799(pMM23) were 34.8 ± 4.3, not detected, 12.3 ± 2.4, and 20.4 ± 0.7 U/mg of protein, respectively.

It can therefore be concluded that the SOD deficiency in *E. coli* was complemented by the *sodA* gene from *C. melassecola*.

Purification and biochemical characterization of SOD. To obtain information on the characteristics of the *C. melassecola*

TABLE 2. Purification of SOD from cell extracts of *C. melassecola*

Fraction	Vol (ml)	Total amt (mg) of protein	Total activity (U)	Sp act (U mg^{-1})	Recovery of activity (%)	Purification (fold)
Cytosoluble	28	227	10,200	45	100	1
$(NH_4)_2SO_4$	15.8	4.9	5,900	1,200	58	27
Bioscale Q2	0.5	0.31	1,300	4,100	13	91
Sephacryl S300	0.54	0.09	380	3,900	4	87

SOD, it was purified as described in Materials and Methods from the wild-type strain. A representative scheme for purification is given in Table 2. The isolated protein was estimated to be pure from SDS-PAGE analysis (Fig. 2). The SOD specific activity of the purified protein was estimated to 3,900 U/mg of protein. The amino acid sequences of the N terminus and two internal peptides isolated from the purified protein were determined (see below). These sequences unambiguously confirmed that the purified protein corresponded to an SOD. The molecular weight of native SOD was estimated to approximately 80,000 from gel filtration chromatography. Its monomeric molecular weight, determined by SDS-PAGE, was 24,000 (Fig. 2). Atomic absorption spectrometry for identification of the metal cofactor in the purified protein was carried out. Manganese was clearly identified, and the calculated stoichiometry was 0.43 atom/subunit. This unbalanced stoichiometry could be explained by either release of manganese from the enzyme during purification or manganese limitation in the growth medium. No signal corresponding to the presence of iron was detected.

Nucleotide sequence analysis of the cloned DNA fragment. The nucleotide sequence of a 2,200-bp fragment from pMM8 was determined by a primer walking strategy from both strands by dideoxy chain termination. Computer analysis revealed two complete and one incomplete ORF, as shown in Fig. 3, extending from ATG (bp 1139) to TAA (bp 1741) for ORF1, from ATG (bp 892) to TAA (bp 239) for ORF2, and from ATG (bp 188) to bp 1 for the incomplete ORF3. ORF2 and ORF3 are in the reverse orientation with respect to ORF1. Database searches with the deduced polypeptides of these three ORFs revealed that the amino acid sequence deduced from ORF1 shows significant homology to known Fe- and Mn-SODs (see below), that deduced from ORF2 shows homology to peptide methionine sulfoxide reductases (PMSR; EC 1.8.4.5) from various organisms (see below), and that deduced from the incomplete ORF3 shows homology to *N*-acyl-L-aminoacid hydrolases from the *Campylobacter jejuni* hippuricase family (27). These results indicated that ORF1 may correspond to the *sodA* gene of *C. melassecola* and ORF2 may correspond to the *msrA* gene. ORF3 has not been named.

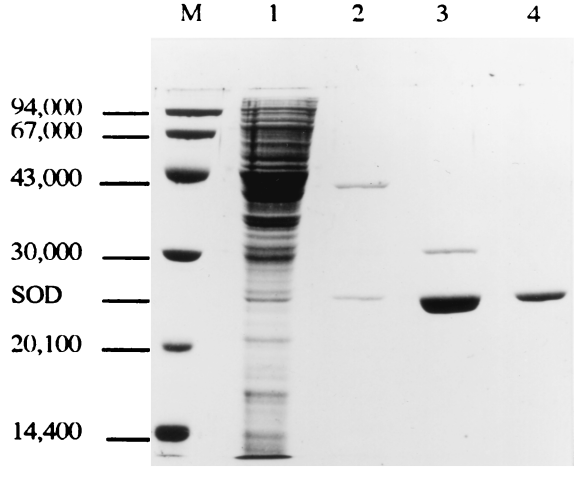

FIG. 2. Purification of SOD from *C. melassecola*. SDS-PAGE of cytosoluble extract from *C. melassecola* (lane 1), extract after ammonium sulfate fractionation (lane 2), and SOD-containing fractions after Bioscale Q2 chromatography (lane 3), and Sephacryl S300 chromatography (lane 4). Lane M, molecular weight standards as described in Materials and Methods.

Analysis of the *sodA* gene. The predicted *sodA* gene product consists of 200 amino acids (Fig. 3), with a molecular weight of 22,104, which is in agreement with the size of the subunit of the purified *C. melassecola* SOD protein (M_r 24,000), as estimated from SDS-PAGE. The G+C content of 57% in the coding region corresponds to a clear preference for C or G at the wobble position, with a codon bias index of 0.79 as calculated according to Malumbres et al. (45). This is consistent with the relative abundance (about 1% of cytosoluble proteins) calculated by the ratio between specific SOD activity in cytosoluble extract (45 U/mg of protein) and for the purified enzyme (3,900 U/mg). In order to confirm the predicted translation initiation site, the N-terminal amino acid sequence of the purified SOD from *C. melassecola* was determined. This sequence was identical to the predicted one with the exception of the initial formyl-methionine, which was missing in the purified enzyme, as described for SODs from various origins (35, 70) and in some *C. glutamicum* proteins (31). The sequences of two internal peptides obtained by trypsin digestion of the purified enzyme were also identical to the deduced sequence. A ribosome-binding site (5′-GAAAGGA-3′), complementary to the 3′ end of the *Brevibacterium lactofermentum* 16S rRNA (3′-AAUCUUUCCUCC-5′) (3), was identified 10 bp upstream from the ATG initiation codon (Fig. 3). Two putative promoter regions with nucleotide sequences close to the consensus sequence for *C. glutamicum* promoters (56) are located upstream from the putative ribosome-binding site. An almost perfect palindromic sequence covers the −35 region from the distal putative promoter. Such a structure could be a binding site for a regulatory factor. Two inverted repeats with putative stable RNA stem-loop structures (ΔG, −61.6 and −87.6 kJ mol^{-1}), located 18 and 88 bp downstream of the stop codon, may represent transcription termination regions. Northern hybridization experiments were performed in order to analyze the size of the *sodA* transcript. Hybridization of *C. melassecola* RNA to an internal *sodA* probe resulted in a single signal at approximately 700 nucleotides (Fig. 4). This size is consistent

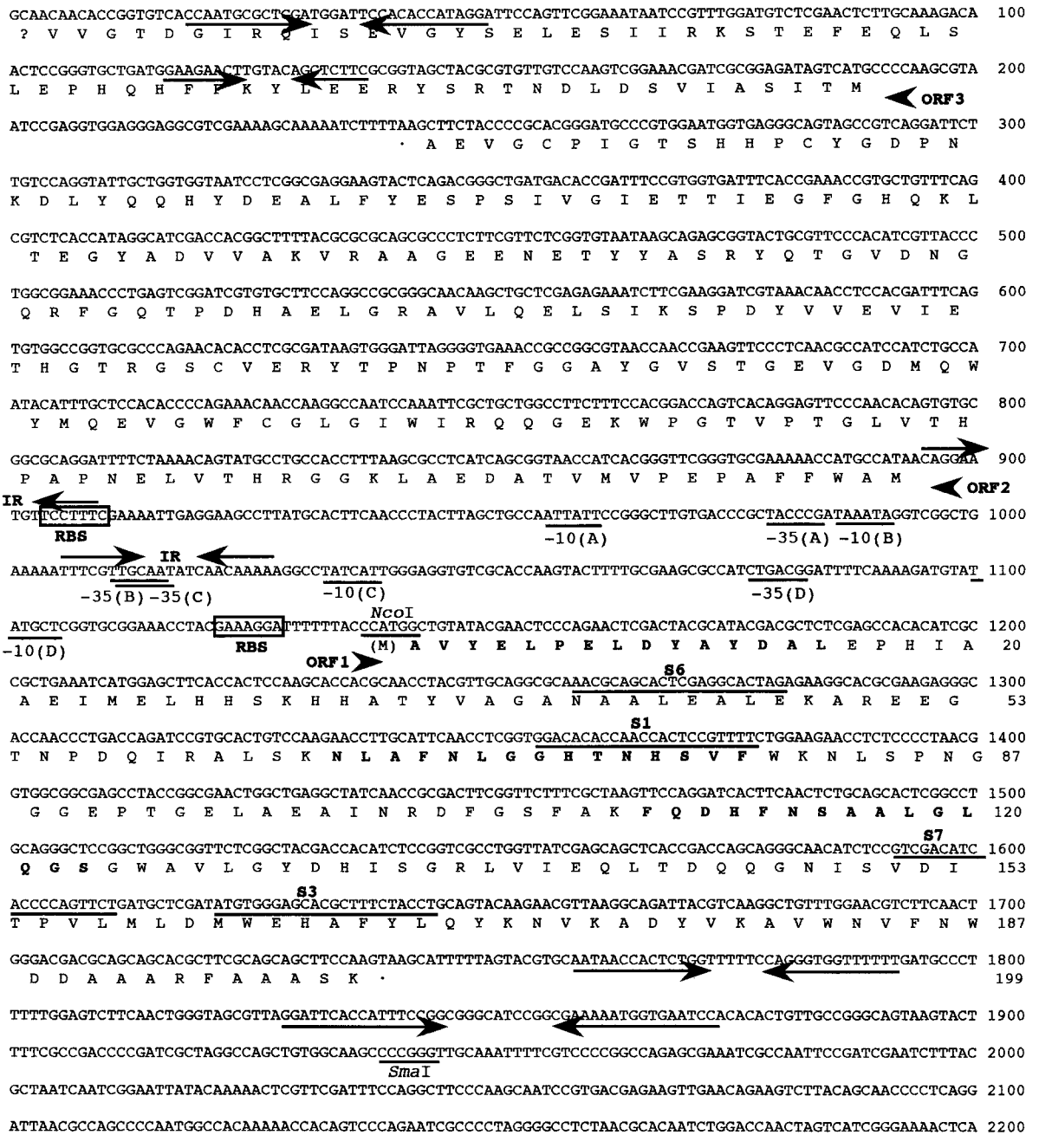

FIG. 3. Nucleotide sequence of *C. melassecola sodA* region. ORF1 corresponds to the SOD and ORF2 to the PMSR encoding sequences; ORF3 is incomplete. The nucleotide sequence corresponds to the *sodA* coding and to the *msrA*-ORF3 noncoding strand. The deduced amino acid sequences are given below the nucleotide sequence. Amino acids that were determined by amino acid sequencing of the purified *C. melassecola* SOD are indicated in bold. Putative ribosome-binding sites (RBS) are boxed, and possible promoter regions are underlined. The two inverted sequences (IR) in the promoter region and the putative strem-loop structures downstream of the ORFs are shown with arrows. The *Nco*I and *Sma*I restriction sites used for pMM23 construction and the locations of PCR primers are underlined (5′-3′ orientation for S6 and S1, 3′-5′ orientation for S7 and S3).

with the translation initiation and termination regions described above and indicates that the *sodA* gene is monocistronic.

Analysis of the deduced SOD amino acid sequence from *C. melassecola*. Comparison of the deduced SOD amino acid sequence with protein sequences from databases using the National Center for Biotechnology Information Blast program (2) revealed high similarity to Fe- and Mn-SODs of prokaryotic and eukaryotic origin. The highest scores were obtained with deduced partial sequences of SODs from the pathogenic *Corynebacterium diphtheriae* and *Corynebacterium pseudodiphtheriticum* species (81% identity) (86) and from the closely

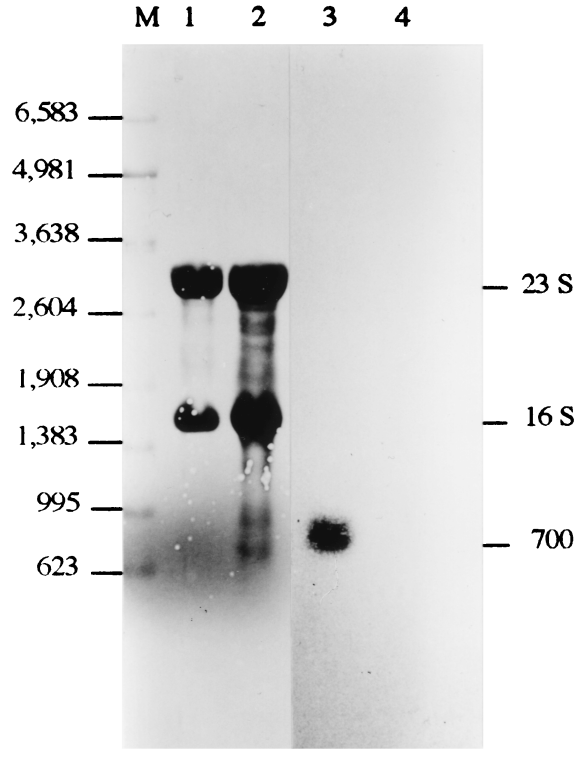

FIG. 4. Northern analysis of the *C. melassecola sodA* gene. RNA was extracted from wild-type *C. melassecola* (lanes 1 and 3) and from the SOD-deficient *C. melassecola* strain CGL10016 (lanes 2 and 4). RNAs were monitored either with a radioactively labeled *sodA* internal probe (lanes 3 and 4) or by methylene blue staining (lanes 1 and 2) as described in Materials and Methods. The positions of RNA standards (Promega) are given (lane M) (in nucleotides).

related *Mycobacterium* species (61% identity with *Mycobacterium leprae* Mn-SOD). Homology was higher with mitochondrial Mn-SODs (54% identity with human Mn-SOD) than with other bacterial species like *Bacillus stearothermophilus* (51% identity) and *E. coli* Mn-SOD (42%) and Fe-SOD (40%). The 12 strictly conserved residues in Fe/Mn-SODs (33), including the four metal-binding residues His_{27}, His_{76}, Asp_{160}, and His_{164} (*C. melassecola* SOD numbering), could be identified. Among the residues involved in metal selectivity, Met_{24}, Leu_{26}, Gly_{71}, Gly_{72}, His_{73}, Phe_{79}, Gln_{145}, and Gln_{169} are predicted to be discriminant for an Mn-dependent enzyme (37, 55). Manganese as a cofactor was clearly identified in the purified *C. melassecola* enzyme by atomic adsorption spectrometry, as described previously.

The predicted folding profile of the *C. melassecola* SOD subunit with α-helices in the N-terminal region and β-sheets together with α-helices in the C-terminal region, as predicted by the PredictProtein program (60, 61), is similar to the typical structure described by crystallographic studies of different Fe/Mn-SODs (10, 16, 67, 68). The molecular mass of the native protein was approximately 80 kDa, as estimated by gel filtration analysis of the purified enzyme, with a monomer molecular weight of approximately 24,000, as seen before (Fig. 2). The active enzyme is thus a homotetramer, as is the case for *Thermus thermophilus* Mn-SOD (67), mitochondrial human Mn-SOD (10), and *Mycobacterium tuberculosis* Fe-SOD (16).

Analysis of the *msrA* and adjacent ORF3 genes and products. The 654-bp-long *msrA* ORF is located only 246 bp upstream from the *sodA* ORF, in the opposite transcriptional orientation (Fig. 3). The predicted *msrA* gene product consists of 217 amino acids, with a calculated molecular weight of 23,892, in agreement with the size of known bacterial PMSRs. The predicted *msrA* gene product showed similarities along its entire length to PMSRs from mammals (50% identity with bovine PMSR [52]) and from bacteria (48% with *E. coli* [58] and 36% with *Streptococcus pneumoniae* [79]). A codon bias index of 0.48 was calculated for *msrA* as described by Malumbres et al. (45), which may indicate a rather low expression level for this gene. A possible ribosome-binding site with the sequence 5′-GAAAGGA-3′ is located 12 bp upstream from the initiation codon, and two possible promoter regions with reasonable homologies to consensus sequences are located further upstream. Two short inverted repeats, one covering the ribosome-binding site and the other located at the distal −35, corresponding also to a potential −35 for the *sodA* gene (see above), could be regions involved in transcriptional regulation.

No clear transcription termination region for *msrA* could be identified, the free energies of the two putative stem-loop structures located downstream of the stop codon being relatively low (ΔG, −28.9 and −27.2 kJ mol^{-1}). Moreover, these stem-loop structures are located within the coding region of ORF3. The end of the *msrA* coding region and the putative ATG for ORF3 are separated by a short stretch of only 51 nucleotides. ORF3 is not preceded by a typical ribosome-binding site. A codon bias index of 0.39 was calculated as described by Malumbres et al. (45) for the truncated ORF3, which may indicate an expression level for this gene as low as that for *msrA*. The predicted product for the incomplete ORF3 shows significant homologies with *N*-acyl-L-amino acid amidohydrolases from the *C. jejuni* hippuricase family (27), an enzyme of unclear physiological function. These observations raise the question of a possible operon organization. Such a hypothesis was not confirmed, since no transcript was identified by Northern blotting experiments with an *msrA* probe under our experimental conditions.

Disruption of the chromosomal *sodA* gene. To study the physiological effects of *sodA* deficiency, the chromosomal copy of this gene was disrupted in *C. melassecola*. For this purpose, the integrative vector viMM12, carrying an internal fragment of the *sodA* coding region and the *aphIII* gene, which confers resistance to kanamycin, was constructed as described in Materials and Methods. Integration of viMM12 by a single crossing-over event in the *sodA* chromosomal locus led to *sodA* gene disruption, as seen by Southern blotting on several transformants (data not shown). Lack of *sodA* transcription and expression in the disrupted CGL10016 strain was confirmed as follows. In Northern blotting experiments with CGL10016 RNAs, no *sodA* transcript was seen (Fig. 4). Activity staining on native polyacrylamide gels did not reveal the presence of any active SOD (not shown). Furthermore, SOD activity in crude extracts from the disrupted strain was 0.24 ± 0.18, versus 17.4 ± 1 U/mg of protein in crude extracts from the wild-type strain. The residual SOD activity in cell extracts from the disrupted strain probably resulted from the presence of about 0.5% genotypic revertants at the stage of cell harvesting (see below).

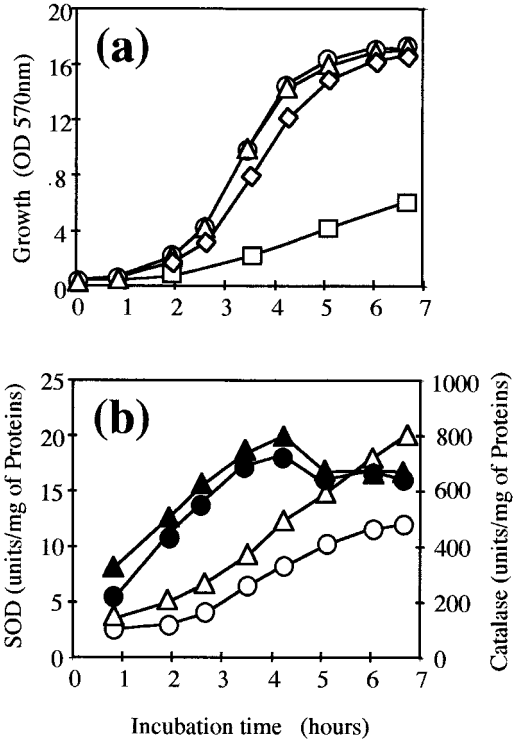

FIG. 5. Effect of paraquat on growth and SOD and catalase activities in *C. melassecola*. (a) Growth of ATCC 17965 (○, △) and SOD-deficient CGL10016 (◇, □) was monitored in BHI or BMCG medium and in BHI with 100 μM paraquat (ATCC 17965, △; CGL10016, □), by measuring OD_{570}. CGL10016 was cultivated in the presence of kanamycin (25 μg/ml). (b) SOD (▲, ●) and catalase (△, ○) activities in ATCC 17965 crude extracts were measured as described in Materials and Methods in the presence (▲, △) and absence (●, ○) of 100 μM paraquat in BHI medium. Activity values are the means of at least three experiments that differed by less than 20%.

Effect of *sodA* disruption on growth. Various growth characteristics of the SOD-proficient wild-type *C. melassecola* strain ATCC 17965 and the corresponding SOD-deficient strain CGL10016 were compared.

The wild-type strain showed pink pigmentation after growth on BHI plates, whereas the CGL10016 mutant remained white. This indicated an SOD-dependent alteration in the biosynthesis or reduction level of a pigment in the mutant strain.

Exponential growth of the *sodA* mutant was only slightly impaired in BHI rich medium as well as in BMCG chemically defined medium without amino acid. In the two media, the mutant strain had a generation time only 10 min longer than that of the wild type (60 versus 50 min) (Fig. 5a). The mutant strain reached the wild-type growth rate after transformation with pMM23 (SOD specific activity of 32 ± 2 U/mg) or addition of the 20 amino acids to the medium.

The prototrophy of the *sodA*-disrupted strain raised the question of the possible presence of another SOD-encoding gene in *C. melassecola*, for example, *sodB*. This seems unlikely for the following reasons. Gardner and Fridovich (23) demonstrated that in a *sodA*-deficient strain of *E. coli*, the residual SOD activity, corresponding to the Fe-SOD encoded by *sodB*, is 30% of the total SOD activity in the wild-type cells, whereas SOD activity is not detected in a *sodA sodB* double mutant. They also demonstrated that the activity of aconitase, known as a superoxide-sensitive enzyme, is lowered to 78% of that of the wild type in a *sodA* mutant and to 30% in a *sodA sodB* double mutant (23). In *C. melassecola*, the SOD activity in the disrupted strain is only 1.4% of that of the wild-type strain and probably results from reversion events, as described below. The specific activity for aconitase in the CGL10016 strain is lowered to 20% of that of the wild-type strain (16 ± 7 and 79 ± 8 nmol min^{-1} mg^{-1}, respectively) when the control isocitrate dehydrogenase activity is not very different (2.47 ± 0.27 and 3.14 ± 0.13 μmol min^{-1} mg^{-1}, respectively).

TABLE 3. Sensitivity of *C. melassecola* strains to oxidizing agents[a]

Inhibitor	Strain	Diam of growth inhibition zone (mm)
Paraquat	ATCC 17965	7
	CGL10016	29
	CGL10016(pMM23)	6
H_2O_2	ATCC 17965	25
	CGL10016	25

[a] Cells were grown on BHI agar plates. Growth inhibition by paraquat or H_2O_2 was tested as described in Materials and Methods. Strains and plasmid pMM23 are described in Table 1.

Effect of *sodA* disruption on oxidative stress response. Responses of the mutant, the pMM23-transformed mutant, and wild-type strains to oxidative stresses generated by paraquat and H_2O_2 were investigated by growth inhibition tests on plates (Table 3) as described in Materials and Methods. Growth of the wild-type strain was not inhibited in the presence of 0.1 mg of paraquat, but the disrupted strain showed a bright inhibition zone. This growth inhibition of the SOD-deficient strain was completely abolished after transformation by pMM23. On the other hand, all strains exhibited the same sensitivity to H_2O_2.

When the wild-type strain was grown in BHI liquid medium in the presence of 100 μM paraquat, growth was not altered and no significant modification in SOD specific activity was observed (Fig. 5). This held true when the paraquat concentation was increased up to 400 μM. On the other hand, catalase was clearly induced when cells were grown in the presence of paraquat (Fig. 5b). This indicates that paraquat efficiently enters cells but does not induce *sodA* expression. At a paraquat concentration of 100 μM, the growth of the disrupted strain was dramatically impaired, indicating that redox cycling was effectively induced and not rescued in the SOD-deficient strain (Fig. 5a).

Effect of *sodA* disruption on viability during stationary phase of growth. To test the effect of SOD deficiency on cell viability after extensive stationary-phase cultivation, cultures of wild-type ATCC 17965 and SOD-deficient CGL10016 *C. melassecola* strains in BHI rich medium and BMCG chemically defined medium were maintained under aeration at 34°C for 6 days. All reached the stationary growth phase in less than 1 day, the OD_{570} then remaining stable at approximatly 20 U (Fig. 6). Viability was estimated at various cultivation times by the CFU/OD ratio. Microscopic observations at each cultivation time did not reveal cellular aggregation.

In BHI rich medium, viability was stable at 1.5 × 10^8

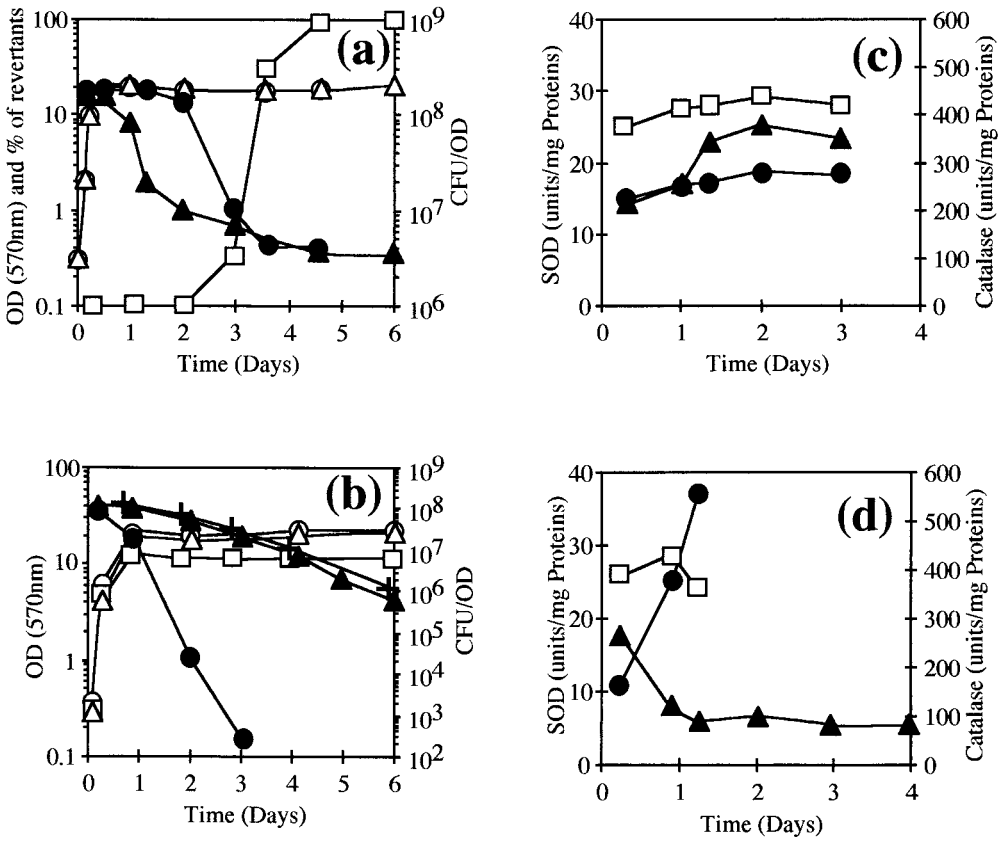

FIG. 6. Viability and SOD and catalase activities of *C. melassecola* during the stationary phase of growth. (a) Growth (○, △), viability (●, ▲), and proportion of phenotypic revertants (□) for SOD-deficient CGL10016 (△, ▲, □), and parental ATCC 17965 (○, ●) strains cultivated in BHI, in the presence or absence of kanamycin (25 μg/ml) for CGL10016. Growth was measured by OD_{570}, and cellular viability was determined by plating on BHI and calculated as CFU/OD. The experiment was done at least three times without significant differences. (b) Growth (○, △, □) and viability (●, ▲, +) determined as described above for ATCC 17965 (○, ●) and CGL10016 (△, ▲) in BMCG (2% glucose) and for ATCC 17965 in BMCG containing only 1% glucose (□, +). Kanamycin (25 μg/ml) was added for CGL10016. (c and d) SOD (□) and catalase (●, ▲) activities measured as described in Materials and Methods, from crude extracts of ATCC 17965 (□, ●) and CGL10016 (▲) strains cultivated in BHI (c) or BMCG with 2% glucose (d) in the presence of kanamycin (25 μg/ml) for CGL10016. Values are the means of at least two experiments that differed by less than 20%.

CFU/OD during logarithmic and early stationary phase for the two strains (Fig. 6a). Viability of the wild-type strain was stable during the first 2 days, then reduced to 2% of the initial value, and remained constant until the end of the experiment. On the other hand, viability of the SOD-deficient strain decreased soon after entry into stationary phase. Cell viability dropped to 5% within the first 2 days and then remained relatively stable.

Loss of viability during these experiments could not be associated with a clear loss of antioxidant activities (Fig. 6c), since catalase specific activity remained relatively constant in the wild-type strain (250 to 280 U/mg) and even increased in the disrupted one (340 to 380 U/mg), and SOD activity was stable in the wild-type strain (26 to 29 U/mg).

Genotypic revertants, phenotypically characterized as pink, kanamycin-sensitive colonies, appeared during the first 2 days of culture of CGL10016. The frequency of reversion increased rapidly to give nearly no SOD-deficient colonies after 4 days. Reversion occurred the same way whether the culture was grown in the presence or absence of kanamycin. Reversion probably resulted from excision of the integrative vector viMM12. As a control, a *C. melassecola malE* mutant (25) and a *dcp* mutant (unpublished data), obtained by a similar disruption strategy, were analyzed in the same conditions, and their insertions remained stable even after 7 days of cultivation.

The same analysis was carried out in BMCG chemically defined medium for both strains (Fig. 6b). After 3 days of cultivation, the viability of the disrupted strain was close to 10% of the initial 1.5×10^8 CFU/OD value and 0.1% after 6 days. The level of genotypic revertants remained below 1% even after 6 days of cultivation. More surprisingly, the viability of the wild-type strain dropped in a more dramatic way: 13% of the initial viability remained after 1 day of cultivation, and only 0.02% remained after 2 days. The strain became nonculturable after 4 days, with more than a 10^8-fold drop in viability. When the glucose concentration in BMCG medium was lowered from 2 to 1%, the wild-type strain viability profile was the same as for the SOD-deficient strain in BMCG containing 2% glucose.

As observed during experiments in BHI, loss of viability during these experiments could not be correlated to the loss of antioxidant activities (Fig. 6d).

DISCUSSION

We identified the *sodA* gene encoding SOD in *C. melassecola* ATCC 17965. As estimated from activity-staining experiments, Northern experiments, SOD and aconitase activity measurements, and response of the wild-type and corresponding *sodA*-disrupted mutant to paraquat, the cloned gene seems to be the unique SOD-encoding gene in this organism. From biochemical experiments on the purified enzyme, SOD from *C. melassecola* was shown to be a homotetramer. From the deduced amino acid sequence, the enzyme belongs to the Mn-dependent SOD family, as experimentally confirmed by atomic adsorption spectrometry. Since SOD from *Mycobacterium tuberculosis* contains iron even though its sequence is closer to that of Mn-SODs than Fe-SODs (85), and since the *Mycobacterium smegmatis* cambialistic enzyme contains both metals (82), it would be interesting to determine if only manganese is present in the SOD of *C. melassecola* after growth in different media or if an iron-substituted enzyme would retain activity.

Putative promoter sequences for the vegetative sigma 70 factor were proposed upstream of the initiation codon, with respect to the promoter consensus sequences from *C. glutamicum* (56). The initiation site for transcription should be determined to clearly identify the actual promoter. The gene was shown to be monocistronic by Northern experiments, and the transcript size is fully compatible with the putative initiation and termination signals of transcription. We were unable to demonstrate regulation of *C. melassecola sodA* gene expression under various growth conditions. No standard binding site for the transcription factors SoxS (41) and Fur (20), involved in the regulation of *sod* genes in other species (29, 72), were found. The SOD specific activity was not significantly different in the wild-type strain grown in the presence or in the absence of paraquat, even if we assumed from experimental data that paraquat-mediated redox cycling readily occurred in this strain. The absence of a change in activity profile upon paraquat addition could be explained either by considering an immediate removal of superoxide radicals by the existing SOD enzyme or by the failure of superoxide radicals to induce *C. melassecola sodA* expression. Nevertheless, the expression of *sodA* could be somehow regulated, as in standard laboratory growth conditions in BHI medium the SOD specific activity was shown to vary. Activity increased during the logarithmic phase of growth and reached a plateau as soon as the culture entered stationary phase, with a maximum at transition phase. It would therefore be interesting to follow the expression of *sodA* in different conditions, in the presence of other stress inducers, for instance, H_2O_2, or when the strain is less likely to produce superoxide radicals, as should be the case under low aeration. It would thus be important for further study of *sodA* expression to put a reporter gene under the control of the upstream sequences of *sodA*.

We identified a second gene, *msrA*, immediately upstream from *sodA*, coding for a putative PMSR (52, 58, 79), whose catalytic activity is the reduction of oxidized methionine residues, a modification leading to functional inactivation of numerous proteins (75). A role for PMSR in protecting against oxidative damage has been described in bacteria (51) and yeasts (50). Thus, the location of the *msrA* gene upstream of *sodA* in *C. melassecola* could be more than just a coincidence. The genes are in opposite transcription orientations, and the two initiation codons are separated by only 246 bp. This kind of divergent organization, with two genes involved in the same physiological process and with coordinate regulation, has often been characterized. For example, it is the case for the *E. coli soxR* and *soxS* genes, involved in superoxide response (81), and for the Fur-regulated *fepA-fes* genes, involved in siderophore production (21). In *M. tuberculosis* and *M. leprae*, the alkyl hydroperoxide reductase and peroxide stress regulator homolog-encoding genes *ahpC* and *oxyR* are divergently transcribed (18). Furthermore, a *sod* gene has been localized upstream from a peroxidase gene in *Helicobacter pylori* (76). Nevertheless, this is the first time that divergent *sod* and *msrA* genes have been reported. Although a *sodA* transcript has been clearly identified in the *C. melassecola* wild-type strain, no *msrA* transcript could be detected, even in the *sodA*-disrupted strain, in which the superoxide level is assumed to be increased. This may be due either to a low transcription level of this gene under our conditions or to poor technology for the extraction and/or detection of large RNA of *C. melassecola* in the case of an operon organization, since *msrA* is immediately followed by ORF3, the physiological role of which is unknown. We now need to look for conditions and methods to detect *msrA* gene expression in *C. melassecola* and to determine if the expression of the divergent *sodA* and *msrA* genes is connected. Northern identification of the *msrA* transcript will also highlight the possible operon organization suggested by the presence of ORF3 immediately downstream of *msrA*.

A *sodA* null mutant was constructed by disruption of the chromosomal gene by an integrative vector carrying a kanamycin resistance gene. Unlike the wild-type strain, the disrupted strain showed an increased sensitivity to superoxide radicals generated by the redox cycling agent paraquat. This indicated that the *sodA* mutation could not be rescued by another activity in *C. melassecola* cells. The growth rate of the disrupted strain was only slightly impaired in BHI rich medium, with a generation time of 60 min, compared to 50 min for the wild-type strain. This is consistant with the behavior of other organisms (13, 36). Much more surprising was the growth of the disrupted strain in BMCG chemically defined medium. Even without supplementary amino acids, its growth rate was the same as in BHI rich medium, whereas the growth of other species of *sod* mutants was dramatically impaired in minimal medium without amino acids (13, 36). Oxidative stress has been proven to exist in the *C. melassecola* mutant strain, as revealed by the decrease in aconitase activity. The prototrophy of the *C. melassecola* SOD-deficient strain could then be explained by a lower sensitivity of amino acid biosynthesis pathways to superoxide radicals generated by aerobic metabolism. Another explanation could be partial compensation for SOD deficiency by either an unidentified enzymatic activity or the presence of an intracellular metabolite or metal ion able to detoxify superoxide radicals. Since the BMCG medium contains 70 μM $FeSO_4$, 10 times the concentration in *E. coli* M63 minimum medium, and since it has been reported that growth in iron-enriched medium can partially compensate for SOD deficiency in *E. coli* (7), iron-mediated compensation of SOD deficiency could be arguable in our case. Note that, as even the wild-type *C. melassecola* ATCC 17965 strain cannot grow in M63, the control experiment was not possible. Carotenoid pigments can

play a role in singlet oxygen and also superoxide scavenging, (8, 12, 49). Carotenoids have been identified in some *Corynebacterium* species (54, 77). Even if it has not been demonstrated that the *C. melassecola* ATCC 17965 pink pigment belongs to this family, its role in superoxide scavenging could be arguable.

While only a small difference in growth rate on BHI medium was observed between wild-type and SOD-deficient strains, they behave in a different way in late stationnary phase with regard to their viability. The viability of the SOD-deficient strain decreased dramatically soon after entry into stationary phase, while the wild-type strain kept a high viability for at least 2 days. Viability of the disrupted strain dropped to 5% of the initial value within 2 days of culture, and almost no *sodA* mutant cells could be recovered after 4 days, when close to 100% of the population consisted of genotypic revertants. Viability loss in SOD-deficient *C. melassecola* is not surprising, since the same type of behavior has been described for other organisms (6, 14, 43, 48), but it still remains unclear why the viability of the wild-type strain decreased after 2 days of culture to reach only 2% of the initial value after 4 days.

When viability was followed in BMCG chemically defined medium, the behavior of the two strains was much more surprising. Viability of the SOD-deficient strain decreased less rapidly than in BHI medium, but continued to decrease for 6 days, while no real increase in reversion was observed, contrary to the behavior in BHI. The most important difference concerns the evolution of viability of the wild-type strain. Viability loss was so dramatic that no viable cells could be recovered after 4 days of cultivation. As the viability profile of the wild-type strain was similar to that of the disrupted strain when the initial glucose concentration was lowered from 2 to 1%, we can conclude that this dramatic loss of viability was the result of an excess of glucose, by a physiological mechanism that is still to be defined, and which does not take place, or takes place to a lesser extent, in the SOD-deficient strain.

Even if wild-type and SOD-deficient strains do not behave in the same way in BHI rich medium and in BMCG chemically defined medium concerning viability, it appeared that loss of viability during the culture cannot be attributed to a decrease in SOD or catalase antioxidant activities. Moreover, catalase activity increased in the SOD-deficient strain in BHI and SOD-proficient strain in BMCG, but only after viability started to decrease.

We have to consider that nonviable cells, as determined by our viability test, could in fact be viable but noncultivable cells, or in a so-called dormant state (19, 38). Nevertheless, this is the first time that a SOD-deficient strain has shown a selective advantage over a wild-type strain. Efforts will now be engaged to understand this at the metabolic level.

ACKNOWLEDGMENTS

This work was supported by grant BIO4-CT96-0145 within the 4th Framework Program of the European Community. M. Merkamm was supported in part by a grant from Eurolysine.

We are grateful to D. Touati for the kind gift of SOD-deficient *E. coli* strains, to A. Boussac for atomic adsorbtion spectrometry experiments, and to M. Blight for critical reading of the manuscript.

REFERENCES

1. **Alcendor, D. J., G. D. Chapman, and B. L. Beaman.** 1995. Isolation, sequencing and expression of the superoxide dismutase-encoding gene (*sod*) of *Nocardia asteroides* strain GUH-2. Gene **164:**143–147.
2. **Altschul, S. F., T. L. Madden, A. A. Schaffer, J. Zhang, Z. Zhang, W. Miller, and D. J. Lipman.** 1997. Gapped BLAST and PSI-BLAST: a new generation of protein database search programs. Nucleic Acids Res. **25:**3389–3402.
3. **Amador, E., J. M. Castro, A. Correia, and J. F. Martin.** 1999. Structure and organization of the *rrnD* operon of '*Brevibacterium lactofermentum*': analysis of the 16S rRNA gene. Microbiology **145:**915–924.
4. **Battistoni, A., F. Pacello, S. Folcarelli, M. Ajello, G. Donnarumma, R. Greco, M. G. Ammendolia, D. Touati, G. Rotilio, and P. Valenti.** 2000. Increased expression of periplasmic Cu,Zn superoxide dismutase enhances survival of *Escherichia coli* invasive strains within nonphagocytic cells. Infect. Immun. **68:**30–37.
5. **Beck, B. L., L. B. Tabatabai, and J. E. Mayfield.** 1990. A protein isolated from *Brucella abortus* is a Cu-Zn superoxide dismutase. Biochemistry **29:** 372–376.
6. **Benov, L., and I. Fridovich.** 1995. A superoxide dismutase mimic protects *sodA sodB Escherichia coli* against aerobic heating and stationary-phase death. Arch. Biochem. Biophys. **322:**291–294.
7. **Benov, L., and I. Fridovich.** 1998. Growth in iron-enriched medium partially compensates *Escherichia coli* for the lack of manganese and iron superoxide dismutase. J. Biol. Chem. **273:**10313–10316.
8. **Black, H. S.** 1998. Radical interception by carotenoids and effects on UV carcinogenesis. Nutr. Cancer **31:**212–217.
9. **Bonamy, C., A. Guyonvarch, O. Reyes, F. David, and G. Leblon.** 1990. Interspecies electro-transformation in corynebacteria. FEMS Microbiol. Lett. **66:**263–269.
10. **Borgstahl, G. E., H. E. Parge, M. J. Hickey, W. F. J. Beyer, R. A. Hallewell, and J. A. Tainer.** 1992. The structure of human mitochondrial manganese superoxide dismutase reveals a novel tetrameric interface of two 4-helix bundles. Cell **71:**107–118. (Erratum, **72:**476, 1993.)
11. **Brosius, J.** 1988. Expression vectors employing lambda-, *trp*-, *lac*- and *lpp*-derived promoters, p. 205–225. *In* R. L. Rodriguez and D. T. Denhardt (ed.), Vectors: a survey of molecular cloning vectors and their uses. Butterworth, Boston, Mass.
12. **Carbonneau, M. A., A. M. Melin, A. Perromat, and M. Clerc.** 1989. The action of free radicals on *Deinococcus radiodurans* carotenoids. Arch. Biochem. Biophys. **275:**244–251.
13. **Carlioz, A., and D. Touati.** 1986. Isolation of superoxide dismutase mutants in *Escherichia coli*: is superoxide dismutase necessary for aerobic life? EMBO J. **5:**623–630.
14. **Clements, M. O., S. P. Watson, and S. J. Foster.** 1999. Characterization of the major superoxide dismutase of *Staphylococcus aureus* and its role in starvation survival, stress resistance, and pathogenicity. J. Bacteriol. **181:** 3898–3903.
15. **Cocaign-Bousquet, M., A. Guyonvarch, and N. D. Lindley.** 1996. Growth rate-dependent modulation of carbon flux through central metabolism and the kinetic consequences for glucose-limited chemostat cultures of *Corynebacterium glutamicum*. Appl. Environ. Microbiol. **62:**429–436.
16. **Cooper, J. B., K. McIntyre, M. O. Badasso, S. P. Wood, Y. Zhang, T. R. Garbe, and D. Young.** 1995. X-ray structure analysis of the iron-dependent superoxide dismutase from *Mycobacterium tuberculosis* at 2.0 angstrom resolution reveals novel dimer-dimer interactions. J. Mol. Biol. **246:**531–544.
17. **Delaunay, S., D. Uy, M. F. Baucher, J. M. Engasser, A. Guyonvarch, and J. L. Goergen.** 1999. Importance of phosphoenolpyruvate carboxylase of *Corynebacterium glutamicum* during temperature triggered glutamic acid fermentation. Metabolic Eng. **1:**334–343.
18. **Dhandayuthapani, S., M. Mudd, and V. Deretic.** 1997. Interactions of OxyR with the promoter region of the *oxyR* and *ahpC* genes from *Mycobacterium leprae* and *Mycobacterium tuberculosis*. J. Bacteriol. **179:**2401–2409.
19. **Dick, T., B. H. Lee, and B. Murugasu-Oei.** 1998. Oxygen depletion induced dormancy in *Mycobacterium smegmatis*. FEMS Microbiol. Lett. **163:**159–164.
20. **Escolar, L., J. Perez-Martin, and V. de Lorenzo.** 1998. Binding of the *fur* (ferric uptake regulator) repressor of *Escherichia coli* to arrays of the GATAAT sequence. J. Mol. Biol. **283:**537–547.
21. **Escolar, L., J. Perez-Martin, and V. de Lorenzo.** 1998. Coordinated repression in vitro of the divergent *fepA-fes* promoters of *Escherichia coli* by the iron uptake regulation (Fur) protein. J. Bacteriol. **180:**2579–2582.
22. **Fridovich, I.** 1995. Superoxide radical and superoxide dismutases. Annu. Rev. Biochem. **64:**97–112.
23. **Gardner, P. R., and I. Fridovitch.** 1991. Superoxide sensitivity of the *Escherichia coli* aconitase. J. Biol. Chem. **266:**19328–19333.
24. **Goldberg, I., and A. Hochman.** 1989. Three different types of catalases in *Klebsiella pneumoniae*. Arch. Biochem. Biophys. **268:**124–128.
25. **Gourdon, P., M.-F. Baucher, N. D. Lindley, and A. Guyonvarch.** 2000. Cloning of the malic enzyme gene from *Corynebacterium glutamicum* and role of the enzyme in lactate metabolism. Appl. Environ. Microbiol. **66:**2981–2987.
26. **Guillouet, S., and J. M. Engasser.** 1995. Sodium and proline accumulation in *Corynebacterium glutamicum* as a response to an osmotic saline upshock. Appl. Environ. Microbiol. **43:**315–320.
27. **Hani, E. K., and V. L. Chan.** 1995. Expression and characterization of *Campylobacter jejuni* benzoylglycine amidohydrolase (hippuricase) gene in *Escherichia coli*. J. Bacteriol. **177:**2396–2402.
28. **Hanson, R. S., and D. P. Cox.** 1967. Effect of different nutritional conditions

on the synthesis of tricarboxylic acid cycle enzymes. J. Bacteriol. **93:**1777–1787.
29. **Hassett, D. J., H. P. Schweizer, and D. E. Ohman.** 1995. *Pseudomonas aeruginosa sodA* and *sodB* mutants defective in manganese- and iron-cofactored superoxide dismutase activity demonstrate the importance of the iron-cofactored form in aerobic metabolism. J. Bacteriol. **177:**6330–6337.
30. **Heinzen, R. A., M. E. Frazier, and L. P. Mallavia.** 1992. *Coxiella burnetii* superoxide dismutase gene: cloning, sequencing, and expression in *Escherichia coli*. Infect. Immun. **60:**3814–3823.
31. **Hermann, T., G. Wersch, E. M. Uhlemann, R. Schmid, and A. Burkovski.** 1998. Mapping and identification of *Corynebacterium glutamicum* proteins by two-dimensional gel electrophoresis and microsequencing. Electrophoresis **19:**3217–3221.
32. **Hopkin, K. A., M. A. Papazian, and H. M. Steinman.** 1992. Functional differences between manganese and iron superoxide dismutases in *Escherichia coli* K-12. J. Biol. Chem. **267:**24253–24258.
33. **Hunter, T., K. Ikebukuro, W. H. Bannister, J. V. Bannister, and G. J. Hunter.** 1997. The conserved residue tyrosine 34 is essential for maximal activity of iron-superoxide dismutase from *Escherichia coli*. Biochemistry **36:**4925–4933.
34. **Igo, M. M., and R. Losick.** 1986. Regulation of a promoter that is utilized by minor forms of RNA polymerase holoenzyme in *Bacillus subtilis*. J. Mol. Biol. **191:**615–624.
35. **Inaoka, T., Y. Matsumura, and T. Tsuchido.** 1998. Molecular cloning and nucleotide sequence of the superoxide dismutase gene and characterization of its product from *Bacillus subtilis*. J. Bacteriol. **180:**3697–3703.
36. **Inaoka, T., Y. Matsumura, and T. Tsuchido.** 1999. SodA and manganese are essential for resistance to oxidative stress in growing and sporulating cells of *Bacillus subtilis*. J. Bacteriol. **181:**1939–1943.
37. **Jackson, S. M., and J. B. Cooper.** 1998. An analysis of structural similarity in the iron and manganese superoxide dismutases based on known structures and sequences. Biometals **11:**159–173.
38. **Kaprelyants, A. S., J. C. Gottschal, and D. B. Kell.** 1993. Dormancy in nonsporulating bacteria. FEMS Microbiol. Rev. **10:**271–285.
39. **Keele, B. B. J., J. M. McCord, and I. Fridovich.** 1970. Superoxide dismutase from *Escherichia coli* B. A new manganese-containing enzyme. J. Biol. Chem. **245:**6176–6181.
40. **Laemmli, U. K.** 1970. Cleavage of structural proteins during the assembly of the head of bacteriophage T4. Nature **227:**680–685.
41. **Li, Z., and B. Demple.** 1996. Sequence specificity for DNA binding by *Escherichia coli* SoxS and Rob proteins. Mol. Microbiol. **20:**937–945.
42. **Liebl, W., M. Ehrmann, W. Ludwig, and K. H. Schleifer.** 1991. Transfer of *Brevibacterium divaricatum* DSM 20297T, "*Brevibacterium flavum*" DSM 20411, "*Brevibacterium lactofermentum*" DSM 20412 and DSM 1412, and *Corynebacterium glutamicum* and their distinction by rRNA gene restriction patterns. Int. J. Syst. Bacteriol. **41:**255–260.
43. **Longo, V. D., E. B. Gralla, and J. S. Valentine.** 1996. Superoxide dismutase activity is essential for stationary phase survival in *Saccharomyces cerevisiae*: mitochondrial production of toxic oxygen species *in vivo*. J. Biol. Chem. **271:**12275–12280.
44. **Lowry, O. H., N. J. Rosebrough, A. L. Farr, and R. J. Randall.** 1951. Protein measurement with the Folin phenol reagent. J. Biol. Chem. **193:**265–275.
45. **Malumbres, M., J. A. Gil, and J. F. Martin.** 1993. Codon preference in corynebacteria. Gene **134:**15–24.
46. **McCord, J. M., and I. Fridovich.** 1969. Superoxide dismutase: an enzymic function for erythrocuprein (hemocuprein). J. Biol. Chem. **244:**6049–6055.
47. **Meier, B., D. Barra, F. Bossa, L. Calabrese, and G. Rotilio.** 1982. Synthesis of either Fe- or Mn-superoxide dismutase with an apparently identical protein moiety by an anaerobic bacterium dependent on the metal supplied. J. Biol. Chem. **257:**13977–13980.
48. **Melov, S., P. E. Coskun, and D. C. Wallace.** 1999. Mouse models of mitochondrial disease, oxidative stress, and senescence. Mutat. Res. **434:**233–242.
49. **Mortensen, A., L. H. Skibsted, J. Sampson, C. Rice-Evans, and S. A. Everett.** 1997. Comparative mechanisms and rates of free radical scavenging by carotenoid antioxidants. FEBS Lett. **418:**91–97.
50. **Moskovitz, J., B. S. Berlett, J. M. Poston, and E. R. Stadtman.** 1997. The yeast peptide-methionine sulfoxide reductase functions as an antioxidant *in vivo*. Proc. Natl. Acad. Sci. USA **94:**9585–9589.
51. **Moskovitz, J., M. A. Rahman, J. Strassman, S. O. Yancey, S. R. Kushner, N. Brot, and H. Weissbach.** 1995. *Escherichia coli* peptide methionine sulfoxide reductase gene: regulation of expression and role in protecting against oxidative damage. J. Bacteriol. **177:**502–507.
52. **Moskovitz, J., H. Weissbach, and N. Brot.** 1996. Cloning and expression of a mammalian gene involved in the reduction of methionine sulfoxide residues in proteins. Proc. Natl. Acad. Sci. USA **93:**2095–2099.
53. **Nilsson, B., M. Uhlen, S. Josephson, S. Gatenbeck, and L. Philipson.** 1983. An improved positive selection plasmid vector constructed by oligonucleotide mediated mutagenesis. Nucleic Acids Res. **11:**8019–8030.
54. **Ostrovsky, D., G. Diomina, E. Lysak, E. Matveeva, O. Ogrel, and S. Trutko.** 1998. Effect of oxidative stress on the biosynthesis of 2-C-methyl-D-erythritol-2, 4-cyclopyrophosphate and isoprenoids by several bacterial strains. Arch. Microbiol. **171:**69–72.
55. **Parker, M. W., and C. C. Blake.** 1988. Iron- and manganese-containing superoxide dismutases can be distinguished by analysis of their primary structures. FEBS Lett. **229:**377–382.
56. **Patek, M., B. J. Eikmanns, J. Patek, and H. Sahm.** 1996. Promoters from *Corynebacterium glutamicum*: cloning, molecular analysis and search for a consensus motif. Microbiology **142:**1297–1309.
57. **Peyret, J. L., N. Bayan, G. Joliff, T. Gulik-Krzywicki, L. Mathieu, E. Schechter, and G. Leblon.** 1993. Characterization of the *cspB* gene encoding PS2, an ordered surface-layer protein in *Corynebacterium glutamicum*. Mol. Microbiol. **9:**97–109.
58. **Rahman, M. A., H. Nelson, H. Weissbach, and N. Brot.** 1992. Cloning, sequencing, and expression of the *Escherichia coli* peptide methionine sulfoxide reductase gene. J. Biol. Chem. **267:**15549–15551.
59. **Reyes, O., A. Guyonvarch, C. Bonamy, V. Salti, F. David, and G. Leblon.** 1991. 'Integron'-bearing vectors: a method suitable for stable chromosomal integration in highly restrictive corynebacteria. Gene **107:**61–68.
60. **Rost, B., and C. Sander.** 1993. Prediction of protein secondary structure at better than 70% accuracy. J. Mol. Biol. **232:**584–599.
61. **Rost, B., and C. Sander.** 1994. Combining evolutionary information and neural networks to predict protein secondary structure. Proteins **19:**55–72.
62. **Sambrook, J., E. F. Fritsch, and T. Maniatis.** 1989. Molecular cloning: a laboratory manual, 2nd ed. Cold Spring Harbor Laboratory, Cold Spring Harbor, N.Y.
63. **Santos, R., S. Bocquet, A. Puppo, and D. Touati.** 1999. Characterization of an atypical superoxide dismutase from *Sinorhizobium meliloti*. J. Bacteriol. **181:**4509–4516.
64. **Schmidt, H. L., W. Stocklein, J. Danzer, P. Kirch, and B. Limbach.** 1986. Isolation and properties of an H_2O-forming NADH oxidase from *Streptococcus faecalis*. Eur. J. Biochem. **156:**149–155.
65. **Silva, G., S. Oliveira, C. M. Gomes, I. Pacheco, M. Y. Liu, A. V. Xavier, M. Teixeira, J. Legall, and C. Rodrigues-Pousada.** 1999. *Desulfovibrio gigas* neelaredoxin: a novel superoxide dismutase integrated in a putative oxygen sensory operon of an anaerobe. Eur. J. Biochem. **259:**235–243.
66. **Stackebrandt, E., F. A. Rainey, and N. L. Ward-Rainey.** 1997. Proposal for a new hierarchic classification system, *Actinobacteria* classis nov. Int. J. Syst. Bacteriol. **47:**479–491.
67. **Stallings, W. C., K. A. Pattridge, R. K. Strong, and M. L. Ludwig.** 1985. The structure of manganese superoxide dismutase from *Thermus thermophilus* HB8 at 2.4-Å resolution. J. Biol. Chem. **260:**16424–16432.
68. **Stallings, W. C., T. B. Powers, K. A. Pattridge, J. A. Fee, and M. L. Ludwig.** 1983. Iron superoxide dismutase from *Escherichia coli* at 3.1-Å resolution: a structure unlike that of copper/zinc protein at both monomer and dimer levels. Proc. Natl. Acad. Sci. USA **80:**3884–3888.
69. **Storz, G., and J. A. Imlay.** 1999. Oxidative stress. Curr. Opin. Microbiol. **2:**188–194.
70. **Takeda, Y., and H. Avila.** 1986. Structure and gene expression of the *E. coli* Mn-superoxide dismutase gene. Nucleic Acids Res. **14:**4577–4589.
71. **Thompson, J. D., D. G. Higgins, and T. J. Gibson.** 1994. CLUSTAL W: improving the sensitivity of progressive multiple sequence alignment through sequence weighting, position-specific gap penalties and weight matrix choice. Nucleic Acids Res. **22:**4673–4680.
72. **Touati, D.** 1997. Superoxide dismutases in bacteria and pathogen protists, p. 447–493. *In* J. C. Scandalios (ed.), Oxidative stress and molecular biology of antioxidant defenses. Cold Spring Harbor Laboratory, Cold Spring Harbor, N.Y.
73. **Touati, D., M. Jacques, B. Tardat, L. Bouchard, and S. Despied.** 1995. Lethal oxidative damage and mutagenesis are generated by iron in Δ*fur* mutants of *Escherichia coli*: protective role of superoxide dismutase. J. Bacteriol. **177:**2305–2314.
74. **Ukeda, H., S. Maeda, T. Ishii, and M. Sawamura.** 1997. Spectrophotometric assay for superoxide dismutase based on tetrazolium salt 3′-1-[(phenylamino)-carbonyl]-3, 4-tetrazolium-bis(4-methoxy-6-nitro)benzenesulfonic acid hydrate reduction by xanthine-xanthine oxidase. Anal. Biochem. **251:**206–209.
75. **Vogt, W.** 1995. Oxidation of methionyl residues in proteins: tools, targets, and reversal. Free Radic. Biol. Med. **18:**93–105.
76. **Wan, X. Y., Y. Zhou, Z. Y. Yan, H. L. Wang, Y. D. Hou, and D. Y. Jin.** 1997. Scavengase p20: a novel family of bacterial antioxidant enzymes. FEBS Lett. **407:**32–36.
77. **Weeks, O. B., and A. G. Andrewes.** 1970. Structure of the glycosidic carotenoid corynexanthin. Arch. Biochem. Biophys. **137:**284–286.
78. **Wilkinson, M., J. Doskow, and S. Lindsey.** 1990. RNA blots: staining procedures and optimization of conditions. Nucleic Acids Res. **19:**679.
79. **Wizemann, T. M., J. Moskovitz, B. J. Pearce, D. Cundell, C. G. Arvidson, M. So, H. Weissbach, N. Brot, and H. R. Masure.** 1996. Peptide methionine sulfoxide reductase contributes to the maintenance of adhesins in three major pathogens. Proc. Natl. Acad. Sci. USA **93:**7985–7990.
80. **Wu, C. H., J. J. Tsai-Wu, Y. T. Huang, C. Y. Lin, G. G. Lioua, and F. J. Lee.** 1998. Identification and subcellular localization of a novel Cu,Zn superoxide dismutase of *Mycobacterium tuberculosis*. FEBS Lett. **439:**192–196.
81. **Wu, J., and B. Weiss.** 1991. Two divergently transcribed genes, *soxR* and

soxS, control a superoxide response regulon of *Escherichia coli*. J. Bacteriol. **173:**2864–2871.
82. **Yamakura, F., K. Kobayashi, S. Tagawa, A. Morita, T. Imai, D. Ohmori, and T. Matsumoto.** 1995. pH-dependent activity change of superoxide dismutase from *Mycobacterium smegmatis*. Biochem. Mol. Biol. Int. **36:**233–240.
83. **Yost, F. J. J., and I. Fridovich.** 1973. An iron-containing superoxide dismutase from *Escherichia coli*. J. Biol. Chem. **248:**4905–4908.
84. **Youn, H. D., E. J. Kim, J. H. Roe, Y. C. Hah, and S. O. Kang.** 1996. A novel nickel-containing superoxide dismutase from *Streptomyces* spp. Biochem. J. **318:**889–896.
85. **Zhang, Y., R. Lathigra, T. Garbe, D. Catty, and D. Young.** 1991. Genetic analysis of superoxide dismutase, the 23 kilodalton antigen of *Mycobacterium tuberculosis*. Mol. Microbiol. **5:**381–391.
86. **Zolg, J. W., and S. Philippi-Schulz.** 1994. The superoxide dismutase gene, a target for detection and identification of mycobacteria by PCR. J. Clin. Microbiol. **32:**2801–2812.